BCSJ Bulletin of the Chemical Society of Japan

Recent Advances in Chiral Plasmonics – Towards Biomedical Applications

Jatish Kumar* and Luis M. Liz-Marzán*

Advance Publication on the web October 10, 2018
doi:10.1246/bcsj.20180236

Recent Advances in Chiral Plasmonics – Towards Biomedical Applications

Jatish Kumar[1]* and Luis M. Liz-Marzán[1,2]*

[1]CIC biomaGUNE and CIBER-BBN, Paseo de Miramón 182, 20014 Donostia-San Sebastián, Spain

[2]Ikerbasque, Basque Foundation for Science, 48013 Bilbao, Spain

E-mail: jatishkumar@cicbiomagune.es; llizmarzan@cicbiomagune.es

Jatish Kumar

Jatish Kumar is a Marie Curie postdoctoral researcher in Prof. Luis M. Liz-Marzán's group in Spain. He obtained his Ph.D. in chemistry from CSIR-NIIST, India, in 2012 under the supervision of Prof. K. George Thomas, and worked as a JSPS postdoctoral fellow in Prof. Tsuyoshi Kawai´s group at NAIST, Nara, Japan. His research interests include synthesis and assembly of nanomaterials, and the mechanistic investigation of chirality at nanoscale.

Luis M. Liz-Marzán

PhD from the University of Santiago de Compostela (1992) and was a postdoc at Utrecht University and visiting professor at various universities and research centers worldwide. After holding a chair in Physical Chemistry at the University of Vigo (1995–2012), he is currently Ikerbasque Research Professor and Scientific Director of CIC biomaGUNE in San Sebastian. His current interests include nanoparticle synthesis and assembly, nanoplasmonics, and nanoparticle-based sensing and diagnostic tools.

Abstract

The field of chirality has seen a strong rejuvenation due to the observation of nanoscale chirality in plasmonic nanoparticles. This account presents recent advances in the field of plasmonic chirality. The various top-down and bottom-up methods adopted for the synthesis of optically active plasmonic nanomaterials are briefly discussed. After achieving significant progress in the synthesis and mechanistic understanding of chirality at the nanoscale, the major focus of researchers is currently set on finding suitable applications for the synthesized nanomaterials. While different applications such as circular polarizers, chiral sensing and catalysis have been proposed, we propose that plasmon-enhanced chiral signals have great potential for use in the detection and therapy of diseases. We therefore introduce recent developments in the use of chiral plasmonic responses in the biomedical field.

Keywords: chiral plasmons, metal nanoparticles, biosensing

1. Introduction

Chirality is a fundamental property associated with the symmetry of molecules, but also of nanoparticles and macroscopic objects. In terms of symmetry elements, a chiral object does not possess inversion symmetry or mirror planes. Hence, an object is termed chiral if it cannot be superimposed on its mirror image by simple rotations or translations. Each of such non-superimposable mirror images in molecular systems is known as an enantiomer. Enantiomeric forms generally display similar physical properties and are thus difficult to differentiate. The chiral nature of molecules becomes evident by analyzing their response to polarized light, or when they interact with another chiral molecule.

In general, chiral objects are characterized by either their efficiency to rotate the plane of linearly polarized light or to absorb left-handed and right-handed circularly polarized light, to a different extent. A peculiar property of a chiral object is that it shows different complex refractive indices for the two different polarization states of circularly polarized light.[1] The rotation of linearly polarized light with respect to its initial polarization is called optical rotary dispersion (ORD).[2] ORD arises from the difference in the real part of the refractive index, which causes a phase shift between the orthogonal polarizations, leading to the rotation of linearly polarized light. The differential absorption of left- and right-circularly polarized light is known as circular dichroism (CD) and arises due to differences in the imaginary part of the refractive index.[3] CD and ORD basically provide the same information and are associated by Kramers-Kronig transformations.[4] While both techniques have advanced toward analytical applications, the presence of overlapping bands in ORD makes spectral analysis more difficult.[2] Owing to its simplicity and direct correlation to the structure, CD has been widely used to probe the secondary and tertiary structure of biomolecules.[3] Moreover, for specific purposes several variants of CD have been used, which include magnetic CD,[5] fluorescence detected CD,[6] and vibrational CD.[7]

Small chiral molecules are well-known to chemists and optical activity in such organic, inorganic and bio-molecules has been vastly investigated.[8,9] Based on the geometry of the molecular system, molecular chirality has been classified as point, axial, planar or helical. A major drawback with chiral investigations on these systems is that the optical response is, in most cases, very weak. Hence, high concentrations of the analyte are required for the investigation of chiral properties. The field of optical activity has recently seen a revival through the discovery of chiral nanoparticles, e.g. in metal nanostructures, which can achieve optical chirality by inducing asymmetry into their geometry.[10-14] Metal nanoparticles support coherent oscillations of conduction electrons on their surface, which are called surface plasmons.[15-17] When a nanostructure is modified in such a way that it acquires a chiral geometry, the surface plasmons associated with that nanostructure achieve a chiral character in turn, which typically feature improved properties, as compared to molecular systems. An interesting aspect of plasmonic nanomaterials is the extremely large dipole strength associated with their surface plasmon resonances, also giving rise to intense CD signals. In addition, the resonances of individual nanoparticles may couple to each other, giving rise to collective modes extending over the entire assembly. In contrast to molecular systems wherein the degree of interaction is limited, the large-scale dipolar and multipolar interactions in plasmonic

nanoassemblies result in intense chiroptical responses.[18]

2. Synthesis of chiral plasmonic nanostructures

Different methodologies have been adopted by researchers to induce chirality into nanoparticles, including; (i) fabrication of chiral shaped nanomaterials,[19-22] (ii) interaction of chiral molecules with achiral plasmonic nanoparticles leading to induced optical activity in the electronic states of nanoparticles,[23-25] and (iii) organization of achiral plasmonic elements into a chiral geometry, with the aid of chiral molecules or other templates.[26-29] Approaches (i) and (ii) result in individual particles that are inherently chiral, whereas approach (iii) gives rise to nanoparticle assemblies with a collective chiral geometry. The vast majority of chiral plasmonic structures reported so far fall in one of these categories, and strong chiroptical responses have been achieved. Optical activity in chiral molecule-achiral nanoparticle complexes is induced through an exciton-plasmon coupling mechanism, whereas the optical response in assembled structures is caused by plasmon-plasmon coupling.[18,23] Chiral nanostructures are usually synthesized following either (i) top-down approach involving nanofabrication techniques such as lithography, or (ii) by bottom-up strategies based on self-assembly. Individual chiral nanostructures have been mainly synthesized by top-down techniques such as direct laser writing or electron beam lithography, with impressive results in obtaining structural features such as spirals and helices.[19-22] However, researchers have recently succeeded in the chemical synthesis of asymmetric chiral nanoparticles possessing inherent optical activity.[30,31] On the other hand, chiral nanoparticle assemblies have been mostly fabricated through bottom up approaches.[26-29] Chiral signatures in such self-assembled nanostructures can be modulated through manipulation of parameters such as helical pitch, aspect ratio and overall dimensions.

2.1 Synthesis of inherently chiral nanostructures

Developments in lithographic techniques have unraveled the scope for the fabrication of nanostructures with different geometries. Chiral nanostructures within a wide range of sizes and shapes have also been synthesized using these techniques. In one of the earlier reports, Gansel and co-workers fabricated plasmonic helices by two-photon direct laser writing and subsequent electroplating.[19] The resulting free-standing helices were shown to exhibit plasmonic modes extending over the entire structure. Each of these plasmonic modes had a distinct handedness and predominantly interacted with light of same handedness, whereas light of opposite handedness was blocked by the array of helices. This resulted in high transmittance for right circularly polarized light from 4000 to 8000 nm. We can thus state that, the helical nanoarray functions as an effective circular polarizer that can convert incident linearly polarized light into circular polarized light. The authors also demonstrated that tapered helices obtained through variation of the diameter and pitch, increased the operation bandwidth of the polarizer.[32] Interestingly, the helical structure and the optical properties associated with it were further optimized by nesting several helices into one another (Figure 1a).[33] Interestingly, these structural changes had a large positive impact on the working principle of the polarizer. While the suppression of transmission for one polarization from a single helix is due to a difference in reflection, the symmetry of three intertwined helices enforces similar reflectance for left- and right-circularly polarized light. Therefore, the observed transmittance difference in this case is purely due to differential absorption, with no scattering contribution.

In one interesting study, Kaschke and co-workers fabricated a complex nanostructure wherein two helices of opposite handedness were stacked on top of each other.[34] The helices were strongly coupled due to the direct ohmic contact, so that the upper spiral blocked light of one polarization, transmitting the other polarization state (Figure 1b). Nevertheless, the energy stored in the fundamental mode of the upper helix was efficiently transferred into the fundamental mode of the lower helix, and subsequently radiated to the far field due to the strong conductive coupling between the two spirals. The combined structure thus functions as a circular polarization converter due to the opposite handedness of the spiral modes. Esposito et al. recently fabricated plasmonic spirals possessing excellent material quality. The spirals exhibited multiple plasmonic modes and pronounced chiral optical signatures in the visible spectral regime. (Figure 1c).[35] The fabricated arrays showed chiral properties at the optical frequencies with extremely high operation bandwidth. Transmission measurements for circularly polarized light exhibited a maximum dissymmetry factor up to 40% in the near infrared region for an array of helices with larger sizes that were fabricated by focused ion beam, and up to 26% in the visible region for the helix array with reduced dimensions fabricated by focused electron beam. While these are some selected examples, a large variety of chiral structures such as staircases, star-shaped apertures, etc. have been fabricated which display enhanced optical activity.

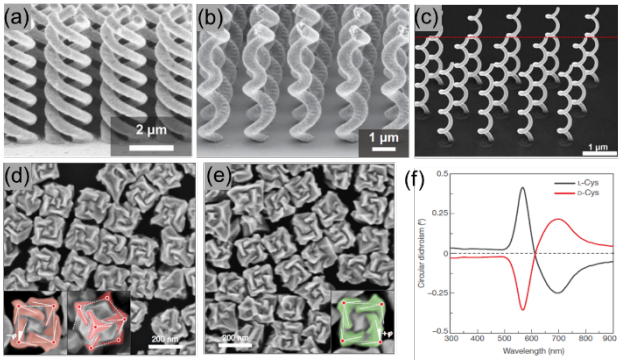

Figure 1. Inherently chiral nanostructures. (a-c) Chiral nanostructures fabricated through top down approach involving lithographic techniques. (a) SEM images of nested plasmonic helices fabricated via a combination of stimulated-emission-depletion direct laser lithography, electrochemical deposition and subsequent wet-etching. Adapted with permission from ref. 33. Copyright 2015, Optical Society of America. (b) SEM image of the gold structures formed after electrochemical deposition of gold on polymer template and subsequent removal polymer via air-plasma etching. Adapted with permission from ref. 34. Copyright 2015, Wiley-VCH. (c) Free-standing metallic spirals fabricated by electron beam–induced deposition. Adapted with permission from ref. 35. Copyright 2014, American Chemical Society. (d-f) Chiral nanoparticles synthesized through bottom-up chemical growth.[30] (d,e) SEM images of the corresponding nanoparticles synthesized using L-cysteine and (d) D-cysteine (e). The insets highlight the tilted edges (solid lines), cubic outline (dashed lines) and tilt angle ($-\phi$ or $+\phi$). (f) CD spectra of chiral nanoparticles synthesized using L-cysteine (black) and D-cysteine (red). Adapted with permission from ref. 30. Copyright 2018, Nature Publishing Group.

While most chiral shaped plasmonic nanostructures are synthesized using lithographic techniques, recent attempts have succeeded in synthesizing inherently chiral plasmonic nanoparticles through bottom-up strategies. Nam and coworkers demonstrated the growth of chiral gold nanoparticles in solution,

using amino acids and peptides as ligands that control the optical activity and chiral plasmonic resonance.[30] The authors attributed the major factor driving the chiral geometry to the formation of high-Miller-index chiral surfaces in the nanoparticles during growth. The enantioselective interactions at the interface between the nanoparticle and amino acid/peptide led to asymmetric evolution of the nanoparticles and the formation of helicoidal morphologies exhibiting intense optical activity (anisotropy factors as high as 0.2) at the plasmon wavelength (Figure 1d-f). The large anisotropy factor of these helicoidal nanoparticles enabled circular polarization dependent color changes that could be distinguished macroscopically. In another interesting report, Kuang and coworkers synthesized chiral Au@AgAu yolk–shell nanorods using chiral D/L-penicillamine decorated Au nanorods as cores with strong plasmon-induced CD signals in the visible spectral range.[31] The intensity and wavelength of the CD signal was successfully modified by tuning various parameters, such as the concentration of D/L-penicillamine, the size of the nanogap, and the aspect ratio of the nanorods.

2.2 Template-based synthesis of chiral nanoassemblies

In addition to the synthesis of intrinsically chiral nanostructures, chiral plasmons can also be generated through the coupling between plasmon modes of interacting nanoparticles. This method involves the assembly of nanoparticles from the lowest geometry (dimer) to large assemblies with varying geometries. The most common strategy involves using a template to assist the assembly of nanoparticles into chiral superstructures with collective properties deriving from interparticle coupling. Versatile templates have been designed to adsorb nanoparticles onto their surface through covalent or non-covalent interactions. One of the first observations of plasmonic chirality involved silver nanoparticles grown on a double stranded DNA template.[36] Since then, DNA has been extensively used for the

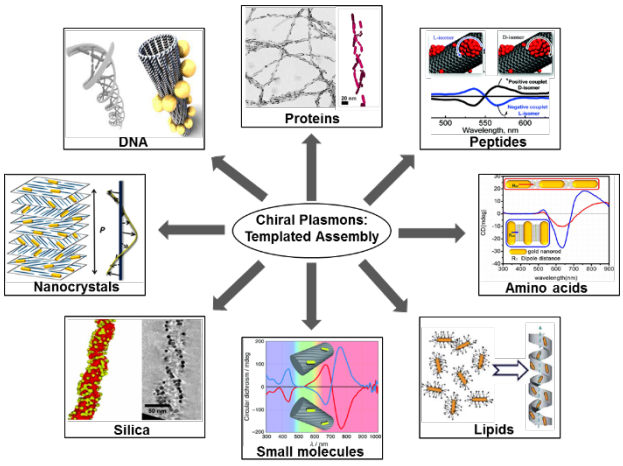

Figure 2. Chirality induced through template-driven assembly of nanoparticles. Directed assembly of nanoparticles using DNA,[40] proteins,[48] peptides,[41] amino acids,[44] lipids,[45] small molecules,[42] silica[47] and cellulose nanocrystals[46] as the chiral templates to drive the assembly of nanoparticles, and for the generation of chiral plasmons. Adapted from the cited papers with permission from American Chemical Society, Wiley-VCH, Royal Society of Chemistry and the National Academy of Sciences.

assembly of nanoparticles and generation of chiral plasmonic structures.[26,27,37,38] For details on the use of DNA-based chiral plasmonic nanostructures, readers are referred to recent reviews on this topic.[39,40] Bisignate mirror image CD signals at the surface plasmon frequency have also been observed for Au nanoparticle clusters adsorbed on D- and L-diphenylalanine peptide nanotubes.[41] In a further development, chiral supramolecular fibers made of anthraquinone-based oxalamide were used by Guerrero-Martínez et al., to assemble anisotropic Au nanorods into imperfect helical structures, which however yielded intense chiral signals.[42] The same group also demonstrated, on the basis of theoretical calculations, that enhanced optical activity should occur for few prolate ellipsoidal particles assembled in a chiral geometry.[42,43] Many other types of templates have been used since, including amino acids,[44] phospholipids,[45] and nanocrystals,[46] as depicted in Figure 2. In a recent report by Oda and co-workers, chiral silica was used for the assembly of Au nanoparticles, being able to tune plasmonic CD signals by varying the pitch and helicity of the template, along with changes in size of the nanoparticles.[47] Kumar et al. recently used protein fibrils as the template for the generation of chiral plasmons, and proposed that the resulting plasmonic CD signals could be used for the detection of Parkinson's and prion diseases (vide infra).[48] We conclude that the template-driven assembly of plasmonic nanoparticles is a versatile tool for the generation of chiral plasmons, since the geometry of nanostructures can be tuned by variations in the template. As a result, chiral plasmonic signals can be modulated in both spectral position and intensity. From the above examples we can see that a significant fraction of the templates used so far are made of biomolecules and hence this technique can find wide application in biodetection, sensing and therapy.

2.3 Synthesis of chiral nanostructures from achiral constituents

Apart from the archetype chiral structures such as the helix or spiral, which exhibit a distinct twist, chiral plasmonic signals can also be obtained from nanosystems without well-defined geometries. Many deformed shapes and assemblies of nanoparticles fall into this category. Even though they do not appear chiral at first sight, the mere fact that they cannot be superimposed with their mirror images renders them optically active. While predicting handedness in helical geometries is usually straightforward, this may not be true for such deformed structures. The nature of the chiral response in such particles will largely depend on the extent of deformation and its influence on the excitation of asymmetric plasmon modes. Although a variety of such nanostructures have been synthesized using lithography,[49-51] we restrict our discussion to the simplest assembling unit, made of nanorod dimers[52-54] formed by stacking individual rods in close proximity. The optical response in such dimers will largely depend on the relative orientation between the dimers and the direction of excitation. As a representative example of this class of nanoparticles, Liu and coworkers designed an optically controlled plasmonic nanosystem comprising two Au nanorods assembled on a reconfigurable DNA origami template.[55] An azobenzene-modified DNA segment acts as the active photoresponsive site on the template. Different conformation states of the nanostructure could be switched by shining light of a specific wavelength, which induces photoisomerization of azobenzene at the localized region. Upon illumination with visible light, the dimer adopts a locked conformation and the CD spectrum exhibits a bisignate peak corresponding to a right-handed system, indicating that the locked plasmonic system features a chiral geometry. In contrast, UV light illumination converted the plasmonic system back into the relaxed state, thereby significantly weakening the CD response (Figure 3a-c). The excellent photoresponsive nature of this plasmonic system was evident from the large modulation of CD intensity between the two states.

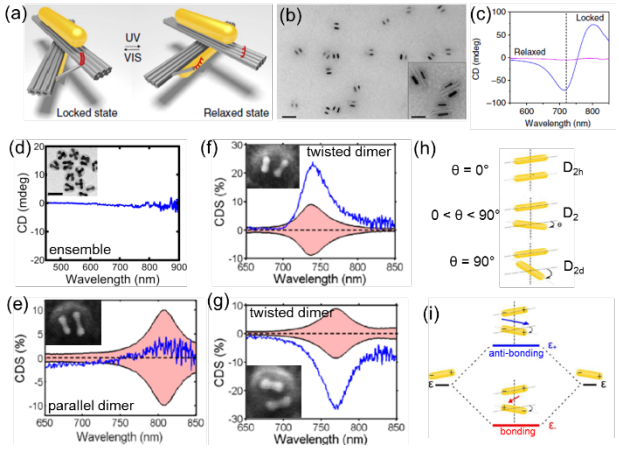

Figure 3. Chirality in nanorod dimers. (a-c) Light-driven 3D plasmonic nanodimer. (a) Schematic representation of the 3D plasmonic dimer regulated by UV and visible light to switch between a right-handed locked state and the relaxed state. (b) TEM images of the plasmonic nanostructures in the locked state (scale bars = 200 and 50 nm in the figure and inset, respectively). (c) Corresponding CD spectra after UV (purple) and visible (blue) light illumination. (d-i) Single particle chiral investigations of nanodimers. Adapted with permission from ref. 55. Copyright 2016, Nature Publishing Group. (d) Ensemble CD spectra of the Au nanodumbbell dimer samples. (e-g) Single particle circular differential scattering spectrum of (e) side-by-side aligned parallel Au nanodumbbell dimer, (f,g) two enantiomers of twisted side-by-side Au nanodumbbells dimers, showing opposite signs. Adapted with permission from ref. 56. Copyright 2016, American Chemical Society. (h) Illustrations of twisted nanorod dimers for 3 twist angles θ, resulting in the associated point groups. (i) Plasmon hybridization diagram for the side-by-side assembled nanorod dimers. Adapted with permission from ref. 57. Copyright 2015, American Chemical Society.

Depending on the specific techniques employed, CD can be used for the measurement of differential extinction, scattering or absorption. Link and co-workers investigated the differential scattering properties of Au nanodumbbell dimers, comprising exclusively achiral constituents.[56] They showed that circular differential scattering analysis of nanostructures at the single particle level could help in deriving a precise correlation between the structure of the dimer and its optical activity. It should be noted that this analysis could be possible only on plasmonic nanoparticles because of the intense optical activity exhibited by these materials, and hence a molecular analogue of this experiment is not feasible at present. In this particular work, ensemble measurements showed no detectable CD signals for either isolated nanodumbbells or dimers (Figure 3d). Even though many dimers were expected to be in chiral configurations, there was no reason to expect predominance of a specific handedness. At the single particle level, scattering spectra of parallel Au nanodumbbell dimers did not showed any meaningful CD activity, due to the achiral nature of such nanostructures (Figure 3e). Interestingly, single-particle measurements on twisted dimers showed significant optical activity, thereby confirming the role of the twisted geometry in inducing chirality. Two different twisted dimers exhibited monosignate line shapes with opposite signs, indicating that they exist as enantiomers with opposite handedness for the direction of the dipoles (Figure 3f,g). According to a plasmon hybridization model, a bisignate CD signal was expected due to the presence of two modes for the chiral dimer geometry; a dominant antibonding mode having a large net dipole and a low-energy bonding mode with a weaker net dipole. However, the bonding mode with opposite handedness to the antibonding mode would be too weak to contribute to the signal in CD scattering spectra, and hence monosignate line shapes were observed because of the dominating scattering response.

Detailed investigations on the circular differential scattering spectra of twisted side-by-side Au nanorod dimers was carried out.[57] This structural symmetry breaking effect, due to size-mismatch between constituent Au nanorods and large twist angles, was found to affect the resulting CD scattering spectrum. It was concluded that, when only scattering is considered, a homo-dimer (dimer composed of nanorods of same sizes) produces a circular differential scattering lineshape that is different from the bisignate response of the corresponding conventional CD spectrum. In contrast, symmetry breaking in a hetero-dimer (where Au nanorods possess different sizes) yields a bisignate circular differential scattering lineshape. The angle between the dimer plays a crucial role in deciding the symmetry parameters of the structure, thereby influencing its optically active plasmon modes. These aspects were further explained with the help of electrodynamic simulations and plasmon hybridization models (Figure 3h,i).

3. Applications of chiral plasmonic nanostructures

Having achieved a reasonable progress in the synthesis and mechanistic investigations of chiral plasmonic nanomaterials, researchers are focusing attention on finding suitable applications for these materials. While various fields have been proposed where chiral plasmonic nanomaterials can find application, these remain a major challenge. One obvious application of chiral nanostructures is the fabrication of metamaterials featuring negative refractive index.[49-51] The refractive index in chiral materials can be defined by the equation $n_{\pm} = \sqrt{\varepsilon\mu} \pm \kappa$, where ε is the electric permittivity, μ is the magnetic permeability, κ is the chirality parameter, and ± corresponds to left- and right-circularly polarized light. Generally, κ is small for chiral molecules and the term becomes insignificant. However, for chiral plasmonic nanomaterials the term can be large enough to drive the total refractive index of the material to negative values for a certain circular polarization. Such negative refractive index metamaterials are gaining interest as potential constituents of cloaking devices and perfect lenses. Another major area where chiral nanomaterials are gaining much attention is biomedicine. We discuss below some recent examples, wherein chiral plasmonic signals were used either to monitor the cell internalization of nanoparticles, for detection of biomolecules and disease biomarkers, or toward novel therapeutic methods.

3.1 Monitoring the cell internalization of nanoparticles

Investigations on the cell internalization of nanoparticles are extremely important when using them as biosensing or therapeutic probes in nanomedicine.[58,59] Development of new techniques to monitor the cell internalization of nanoparticles is an active topic of research pursued in a number of research groups. Working in this direction, Xu and Kotov demonstrated that the chiroptical signals from DNA-bridged nanoparticle dimers could be used to follow the internalization of nanoparticles in mammalian cells.[60] A reversal in the sign of the plasmonic CD signals from negative to positive during transmembrane transport was used to identify internalization (Figure 4a). A large change in electrostatic repulsion between nanoparticles is expected when the dimers move from the interstitial fluid into the cytosol. The change of equilibrium

conformation of the assemblies would in turn result in a spontaneous twisting motion around the DNA bridging the nanoparticles, ultimately leading to a reversal in the chirality. In the case of chiral nanoparticle dimers, the direction of the dipoles establishes the sign of the corresponding CD signals. The twisting motion of the linker during transmembrane transport helped in the reorientation of the nanoparticles, thereby changing the direction of the dipoles constituting the chiral geometry. Such a reorientation of dipoles leads to inversion of the chiral plasmonic signals, thereby helping the authors to successfully distinguish extra- vs. intra-cellular localization of the nanoparticles (Figure 4b,c). The efficiency of the method is such that it can in principle be used for the spectroscopic targeting of plasmonic nanodrugs. The nanorod dimers were further used for photodynamic therapy of malignancies. A drastic increase in the generation of reactive oxygen species, and effective elimination of the cervical cancer cells were observed when circular polarization of incident photons matched the preferential absorption by dimers that were localized inside the cancer cells. The authors have recently extended the strategy to chiral semiconductor CdTe nanoparticles, wherein site-selective in vivo photoinduced cleavage and profiling of DNA was achieved by exciting the sample with light having circular polarization that favors absorption by the nanoparticles.[61]

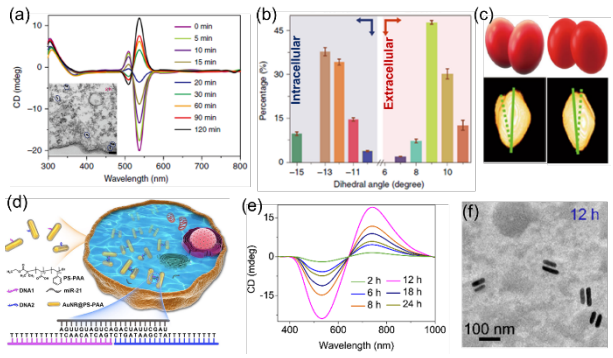

Figure 4. (a-c) Chiral plasmons used to investigate cell internalization of nanoparticles. (a) CD spectra of NP dimers incubated with HeLa cells over a period of 2 h. The inset shows the corresponding TEM images of NP dimers in cells. (b) Statistical analysis of the dihedral angles θ for nanoparticle dimers inside and outside the cell determined from cryo-TEM tomography images. (c) The corresponding TEM tomography images (bottom) and schematics of dimer geometry (top). Adapted with permission from ref. 60. Copyright 2017, Nature Publishing Group. **(d-f) Detection of microRNA in cells.** (d) Schematic illustration of the formation of Au nanorod chiral side-by-side dimers driven by a target microRNA. (e) CD spectra of nanorod-DNA incubated with MCF-7 cells over a period of 24 h. (f) Representative TEM images of assembled nanorod dimers in cell lysates after a time period of 12h. Adapted with permission from ref. 63. Copyright 2018, Wiley-VCH.

3.2 Specific microRNA detection

Chiral plasmonic nanomaterials have been used for the detection of DNA,[62] microRNA,[63,64] cancer biomarkers and certain glycoproteins.[65] In most cases nanoparticle dimers, which are the smallest possible assembling unit, were used for the generation of chiral detection signals. Recently Xu et al. demonstrated that the chiroplasmonic response from Au nanorod dimers can be used for the detection of microRNA inside living cells.[63] Single stranded DNA bound to Au nanorods was used for the selective recognition of specific microRNA sequences. The chiral DNA linker bound to the nanorods would hybridize with a specific microRNA, resulting in the formation of twisted side-by-side Au nanorod dimers (Figure 4d). Unlike achiral linear or parallel dimer geometries, the twisted conformation of nanorod dimers led to a chiral geometry, giving rise to CD signals in the plasmonic region. The sign of the CD signal is determined by the orientation of the nanorods within the dimer. Hence, the formation of dimers was evidenced by intense CD signals in the visible and the near infrared, and could therefore be used for microRNA detection (Figure 4e). The formation of dimers at different stages was confirmed with the help of TEM images (Figure 4f). An increase in the concentration of the target microRNA resulted in an increased degree of dimer formation, thereby enhancing chiroplasmonic signals. As a result, the approach was used for the semi-quantification of target microRNA in cells, by monitoring the optical spectra of nanoplasmonic dimers. The relevance of this technique is related to providing additional insights into the real time monitoring of biomarkers in living cells using plasmonic probes, and can improve the current understanding of cellular RNA-protein interactions.

3.3 Detection of Parkinson's disease

Chiral plasmonic nanostructures exhibit intense optical activity, and can be used for the detection as well as for therapy of certain diseases. We have seen above that by assembling nanostructures, the optical responses can be further enhanced, thereby improving the sensitivity of the potential detection platform. Working in this direction, Kumar et al. recently applied chiroptical effects in Au nanorods to the detection of amyloid fibrils in Parkinson's disease.[48] The different interactions of Au nanorods with infectious fibrils and the stable monomer protein, were used as the basis of the proposed detection platform, so that a clear distinction in the plasmonic CD signals of Au nanorods could be used to differentiate between the monomeric and fibrillar states of the proteins (Figure 5a,b). Monomeric α-synuclein proteins showed no apparent interaction with Au nanorods, thereby remaining CD silent in the plasmonic region. In contrast, the helical nature of the amyloid fibrils could successfully drive the assembly of Au nanorods on their surface via non-covalent interactions, resulting in intense optical activity at the surface plasmon resonance wavelengths. The three-dimensional double helical arrangement of Au nanorods on the surface of the fibrils was confirmed by cryo-electron tomography reconstructions (Figure 5c). Such a three dimensional chiral nanorod arrangement, driven by a chiral template, resulted in the loss of certain symmetry elements, thereby giving rise to CD signals in the plasmonic region. In contrast, no specific arrangement was obtained when protein monomers were bound to nanorods, resulting in CD silent spectra, and therefore enabling the successful differentiation of fibrils from monomers, using plasmonic chirality. Subsequently, the sensing technique was successfully applied to human brain homogenates, showing the possibility to distinguish Parkinson's from healthy brain samples, using chiral plasmonic signals in the visible and near infrared spectral ranges. The technique was further extended to the specific detection of infectious amyloids formed by prion proteins, thereby confirming its wide potential as a detection platform that can be applied to other neurodegenerative diseases.

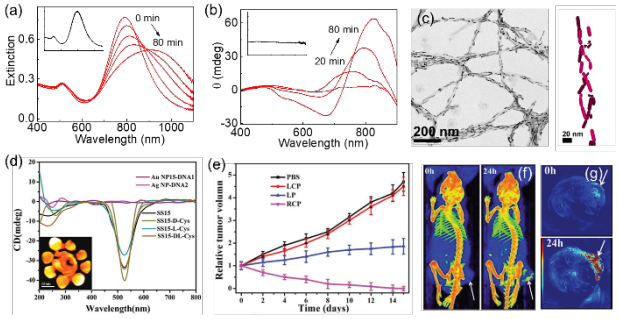

Figure 5. (a-c) Detection of Parkinson's disease using plasmonic chirality. Extinction (a) and CD (b) spectral changes of Au nanorods monitored after the addition of α-synuclein fibrils. Insets show the corresponding spectra in the presence of α-synuclein monomers. (c) TEM and cryo-TEM tomography reconstruction image of Au nanorods-protein nanofiber composite showing the 3D chiral arrangement of Au nanorods. Adapted with permission from ref. 48. Copyright 2018, National Academy of Sciences. **(d-g) Chiral plasmonic nanostructures as efficient photosensitizers.** (d) CD spectra of the satellite nanoassemblies with 20 × 10^{-6} M D-, L- and DL-cysteine modifications. The inset shows a 3D tomography image of the nanoassembly. (e) In vivo relative tumor growth curves under illumination with light of different polarizations. (f) X-ray computed tomography and (g) photoacoustics imaging of HeLa tumor-bearing mice, taken at different time points after injection with satellite nanoassembly. Adapted with permission from ref. 66. Copyright 2017, Wiley-VCH.

3.4 Photosensitizing in Photodynamic Therapy

Photodynamic therapy (PDT) is an efficient, noninvasive, site-selective nanomedicine tool for the local ablation of cancer cells. While a series of photosensitizers, ranging from organic derivatives to nanosystems have been developed, chiral plasmonic nanoparticles are still at an early stage as intracellular PDT agents. In one of the few examples, Kuang and co-workers fabricated DNA-based shell–satellite Au nanoassemblies as chiral photosensitizers.[66] The plasmonic nanostructure, coupled with cysteine enantiomers on its surface, exhibited intense chiroptical signals in the visible region, with preferential absorption for light of specific polarization (Figure 5d). The presence of a chiral molecule such as cysteine can induce asymmetry into the geometry giving rise to plasmonic CD signals. Such chiral nanostructures can selectively absorb light of one circular polarization depending on its geometry. The chiral geometry in case of shell–satellite Au nanoassemblies exhibited better efficiency when excited with light of right circular polarization. Hence, the chiral nanoassemblies showed high efficiency in singlet oxygen generation, with a quantum yield of 1.09 for illumination under right circularly polarized light. A relatively low dose of the chiral photosensitizer could achieve the intracellular reactive oxygen species threshold for PDT, presenting extraordinary efficiency in vitro, compared with traditional drugs. Moreover, in mice treated with the developed chiral assemblies, tumors were completely ablated due to PDT effects (Figure 5e). The remarkable efficiency of the nanostructure under illumination with light of specific circular polarization allowed its use in simultaneous X-ray computed tomography and photoacoustic imaging for tumors, *in vitro* and *in vivo* (Figure 5f,g). Considering the fact that plasmonic nanoparticles are attractive as contrast agents in various imaging platforms, the use of chiral nanostructures can open new avenues toward systems exhibiting better efficiency, as compared to their achiral counterparts.

4. Conclusions and future prospect

Chiral plasmonic nanosystems have gained much attention among researchers working in the field of nanoscience, due to their remarkable optical activity. Advances in nanofabrication techniques have simplified the synthetic routes of complex chiral plasmonic nanosystems. The efficient chirality transfer from chiral biomolecules/templates has additionally permitted the successful synthesis of a wide variety of chiral nanoarchitectures possessing varying optical responses. In addition to isolated nanostructures, resonant interaction between adjacent nanoparticles gives rise to intense optical responses that outweigh their molecular counterparts by few orders in magnitude. Additionally, switching of chiral signals have been realized for plasmonic nanomaterials, with interesting applications in sensing of different analytes, detection of biomolecules and therapy of diseases. On the other hand, the strong dipolar and multipolar coupling in plasmonic nanomaterials have resulted in intense chiroptical signals that enable the detection of analytes at very low concentrations. Applications in the biomedical field have been facilitated by the synthesis of biocompatible nanoparticles, as well as the specificity of the plasmonic chiral signatures. With further advancement in the synthetic protocols, the field of chiral nanoplasmonics is expected to replace its achiral counterparts and will definitely find applications in broader areas.

Acknowledgement

J.K. acknowledges financial support from the European Commission under Marie Sklodowska-Curie Program (H2020-MSCA-IF-2015_708321). L.M.L.-M. acknowledges funding from the Spanish MINECO (Grant no. MAT2017-86659-R).

References

1. A. Rodger, B. Norden, Circular Dichroism and Linear Dichroism, **1997**, Oxford Univ. Press.
2. H. Eyring, H.-C. Liu, D. Caldwell, *Chem. Rev.* **1968**, *68*, 525.
3. K. Nakanishi, N. Berova, R. Woody (Eds.), Circular Dichroism, Principles and Applications, **1994**, VCH, pp. 570.
4. C.A. Erneis, L.J. Oosterhoff, G. Vries, *Proc. Roy. Soc. A* **1967**, *297*, 54.
5. H. Isci, W. R. Mason, *Inorg. Chem.* **1985**, *24*, 271.
6. D. H. Turner, I. Tinoco Jr., M. Maestre, *J. Am. Chem. Soc.* **1974**, *96*, 4340.
7. L.A. Nafie, T.A. Keiderling, P.J. Stephens, *J. Am. Chem. Soc.* **1976**, *98*, 2715.
8. J. R. Brandt, F. Salerno, M. J. Fuchter, *Nat. Rev. Chem.* **2017**, *1*, 0045.
9. J. Kumar, T. Nakashima, T. Kawai, *J. Phys. Chem. Lett.* **2015**, *6*, 3445.
10. M. Hentschel, M. Schäferling, X. Duan, H. Giessen, N. Liu, *Sci. Adv.* **2017**, *3*, e1602735.
11. V. K. Valev, J. J. Baumberg , C. Sibilia, T. Verbiest, *Adv. Mater.* **2013**, *25*, 2517.
12. J. Kumar, K. G. Thomas, L. M. Liz-Marzán, *Chem. Commun.* **2016**, *52*, 12555.
13. J. Cheng, E. H. Hill, Y. Zheng, T. He, Y. Liu, *Mater. Chem. Front.* **2018**, *2*, 662.
14. X. Lan, Q. Wang, *Adv. Mater.* **2016**, *28*, 10499.
15. P. Mulvaney, *Langmuir* **1996**, *12*, 788.
16. L. M. Liz-Marzán, *Mater. Today* **2004**, *7*, 26.
17. R. Yu, L. M. Liz-Marzán, F. J. García de Abajo, *Chem. Soc. Rev.* **2017**, *46*, 6710.
18. R. Thomas, J. Kumar, J. George, M. Shanthil, G. N. Naidu,

R. S. Swathi, K. G. Thomas, *J. Phys. Chem. Lett.* **2018**, *9*, 919.
19. J. K. Gansel, M. Thiel, M. S. Rill, M. Decker, K. Bade, V. Saile, G. von Freymann, S. Linden, M. Wegener, *Science* **2009**, *325*, 1513.
20. H. S. Park, T. T. Kim, H. D. Kim, K. Kim, B. Min, *Nat. Commun.* **2014**, *5*, 5435.
21. Y. Cui, L. Kang, S. Lan, S. Rodrigues, W. Cai, *Nano Lett.* **2014**, *14*, 1021.
22. Y. Fang, R. Verre, L. Shao, P. Nordlander, M. Kall, *Nano Lett.* **2016**, *16*, 5183.
23. A. O. Govorov, Z. Fan, *Nano Lett.* **2010**, *10*, 1374.
24. J. M. Slocik, A. O. Govorov, R. R. Naik, *Nano Lett.* **2011**, *11*, 701.
25. V. A. Gérard, Y. K. Gun'ko, E. Defrancq, A. O. Govorov, *Chem. Commun.* **2011**, *47*, 7383.
26. A. Kuzyk, R. Schreiber, Z. Fan, G. Pardatscher, E.-M. Roller, A. Hogele, F. C. Simmel, A. O. Govorov, T. Liedl, *Nature* **2012**, *483*, 311.
27. X. Lan, X. Lu, C. Shen, Y. Ke, W. Ni, Q. Wang, *J. Am. Chem. Soc.* **2015**, *137*, 457.
28. C. Song, M. G. Blaber, G. Zhao, P. Zhang, H. C. Fry, G. C. Schatz, N. L. Rosi, *Nano Lett.* **2013**, *13*, 3256.
29. S. H. Jung, J. Jeon, H. Kim, J. Jaworski, J. H. Jung, *J. Am. Chem. Soc.* **2014**, *136*, 6446.
30. H.-E. Lee, H.-Y. Ahn, J. Mun, Y. Y. Lee, M. Kim, N. H. Cho, K. Chang, W. S. Kim, J. Rho, K. T. Nam, *Nature* **2018**, *556*, 360.
31. C. Hao, L. Xu, M. Sun, W. Ma, H. Kuang, C. Xu, *Adv. Funct. Mater.* **2018**, *28*, 1802372.
32. J. K. Gansel, M. Latzel, A. Frölich, J. Kaschke, M. Thiel, M. Wegener, Appl. Phys. Lett. 2012, 100, 101109.
33. J. Kaschke, M. Wegener, *Opt. Lett.* **2015**, *40*, 3986.
34. J. Kaschke, L. Blume, L. Wu, M. Thiel, K. Bade, Z. Yang, M. Wegener, *Adv. Opt. Mater.* **2015**, *3*, 1411.
35. M. Esposito, V. Tasco, M. Cuscunà, F. Todisco, A. Benedetti, I. Tarantini, M. De Giorgi, D. Sanvitto, A. Passaseo, *ACS Photonics* **2014**, *17*, 105.
36. G. Shemer, O. Krichevski, G. Markovich, T. Molotsky, I. Lubitz, A. B. Kotlyar, *J. Am. Chem. Soc.* **2006**, *128*, 11006.
37. R. Schreiber, N. Luong, Z. Fan, A. Kuzyk, P. C. Nickels, T. Zhang, D. M. Smith, B. Yurke, W. Kuang, A. O. Govorov, T. Liedl, *Nat. Commun.* **2013**, *4*, 2948.
38. M. J. Urban, P. K. Dutta, P. Wang, X. Duan, X. Shen, B. Ding, Y. Ke, N. Liu, *J. Am. Chem. Soc.* **2016**, *138*, 5495.
39. A. Cecconello, L. V. Besteiro, A. O. Govorov, I. Willner, *Nat. Rev.* **2017**, *2*, 17039.
40. C. Zhou, X. Duan, N. Liu, *Acc. Chem. Res.* **2017**, *50*, 2906.
41. J. George, K. G. Thomas, *J. Am. Chem. Soc.* **2010**, *132*, 2502.
42. A. Guerrero-Martinez, B. Auguie, J. L. Alonso-Gomez, Z. Dzolic, S. Gomez-Graña, M. Zinic, M. M. Cid, L. M. Liz-Marzán, *Angew. Chem. Int. Ed.* **2011**, *50*, 5499.
43. B. Auguie, J. L. Alonso-Gomez, A. Guerrero-Martinez, L. M. Liz-Marzán, *J. Phys. Chem. Lett.* **2011**, *2*, 846.
44. B. Han, Z. Zhu, Z. Li, W. Zhang, Z. Tang, *J. Am. Chem. Soc.* **2014**, *136*, 16104.
45. R.-Y. Wang, H. Wang, X.C. Wu, Y. Ji, P. Wang, Y. Qua, T.-S. Chung, *Soft Matter* **2011**, *7*, 8370.
46. A. Querejeta-Fernández, G. Chauve, M. Methot, J. Bouchard, E. Kumacheva, *J. Am. Chem. Soc.* **2014**, *136*, 4788.
47. J. Cheng, G. L. Saux, J. Gao, T. Buffeteau, Y. Battie, P. Barois, V. Ponsinet, M.-H. Delville, O. Ersen, E. Pouget, R. Oda, *ACS Nano* **2017**, *11*, 3806.
48. J. Kumar, H. Eraña, E. López-Martínez, N. Claes, V. F. Martín, D. M. Solís, S. Bals, A. L. Cortajarena, J. Castilla, L. M. Liz-Marzán, *Proc. Natl. Acad. Sci. USA*, **2018**, *115*, 3225.
49. C. Han, H. M. Leung, C. T. Chan, W. Y. Tam, *Opt. Express* **2015**, *23*, 33065.
50. K. Dietrich, C. Menzel, D. Lehr, O. Puffky, U. Hübner, T. Pertsch, A. Tünnermann, E.-B. Kley, *Appl. Phys. Lett.* **2014**, *104*, 193107.
51. B. Yeom, H. Zhang, H. Zhang, J. I. Park, K. Kim, A. O. Govorov, N. A. Kotov, *Nano Lett.* **2013**, *13*, 5277.
52. X. Lan, Z. Chen, G. Dai, X. Lu, W. Ni, Q. Wang, *J. Am. Chem. Soc.* **2013**, *135*, 11441.
53. W. Ma, H. Kuang, L. Wang, L. Xu, W. -S. Chang, H. Zhang, M. Sun, Y. Zhu, Y. Zhao, L. Liu, C. Xu, S. Link, N. A. Kotov, *Sci. Rep.* **2013**, *3*, 1934.
54. Z. Chen, X. Lan, Y. –C. Chiu, X. Lu, W. Ni, H. Gao, Q. Wang, *ACS Photonics* **2015**, *2*, 392.
55. A. Kuzyk, Y. Yang, X. Duan, S. Stoll, A. O. Govorov, H. Sugiyama, M. Endo, N. Liu, *Nat. Commun.* **2016**, *7*, 10591.
56. K. W. Smith, H. Zhao, H. Zhang, A. Sánchez-Iglesias, M. Grzelczak, Y. Wang, W.-S. Chang, P. Nordlander, L. M. Liz-Marzán, S. Link, *ACS Nano* **2016**, *10*, 6180.
57. L.-Y. Wang, K. W. Smith, S. Dominguez-Medina, N. Moody, J. M Olson, H. Zhang, W.-S. Chang, N. A. Kotov, S. Link, *ACS Photonics* **2015**, *2*, 1602.
58. J. Mosquera, M. Henriksen-Lacey, I. García, M. Martínez-Calvo, J. Rodríguez, J. L. Mascareñas, Luis M. Liz-Marzán, *J. Am. Chem. Soc.* **2018**, *140*, 4469.
59. S. Behzadi, V. Serpooshan, W. Tao, M. A. Hamaly, M. Y. Alkawareek, E. C. Dreaden, D. Brown, A. M. Alkilany, O. C. Farokhzad, M. Mahmoudi, *Chem. Soc. Rev.* **2017**, *46*, 4218.
60. M. Sun, L. Xu, J. H. Banhg, H. Kuang, S. Alben, N. A. Kotov, C. Xu, *Nat. Commun.* **2017**, *8*, 1847.
61. M. Sun, L. Xu, A. Qu, P. Zhao, T. Hao, W. Ma, C. Hao, X. Wen, F. M. Colombari, A. F. de Moura, N. A. Kotov, C. Xu, H. Kuang, *Nat. Chem.* **2018**, *10*, 821.
62. W. Ma, H. Kuang, L. Xu, L. Ding, C. Xu, L. Wang, N. A. Kotov, *Nat. Commun.* **2013**, *4*, 2689.
63. L. Xu, Y. Gao, H. Kuang, L. M. Liz-Marzán, C. Xu, *Angew. Chem. Int. Ed.* **2018**, *57*, 10544.
64. S. Li, L. Xu, W. Ma, X. Wu, M. Sun, H. Kuang, L. Wang, N. A. Kotov, C. Xu, *J. Am. Chem. Soc.* **2016**, *138*, 306.
65. X. Wu, L. Xu, W. Ma, L. Liu, H. Kuang, N. A. Kotov, C. Xu, *Adv. Mater.* **2016**, *28*, 5907.
66. F. Gao, M. Sun, W. Ma, X. Wu, L. Liu, H. Kuang, C. Xu, *Adv. Mater.* **2017**, *29*, 1606864.